An efficient Lumped Mixed Hybrid Finite Element formulation for variably saturated groundwater flow

Benjamin BELFORT[†,*], Fanilo RAMASOMANANA[†], Anis YOUNES[†], and François LEHMANN[†]

[†] *Institut de Mécanique des Fluides et des Solides, Université Louis Pasteur de Strasbourg - CNRS/UMR 7507*

2 rue Boussingault, F- 67000 Strasbourg, France.

Submitted to Vadose Zone Journal

July 2008

* Corresponding author
Institut de Mécanique des Fluides et des Solides
Université Louis Pasteur - CNRS - UMR 7507
2, rue Boussingault, 67000 Strasbourg, France

Tél : 33 390 242 920
Fax : 33 388 614 300
Mail : bbelfort@imfs.u-strasbg.fr

Abstract

Accurate numerical simulation of infiltration in the vadose zone remains a challenge, especially when very sharp fronts are modeled. In this work, we use the Mixed Hybrid Finite Element (MHFE) method which allows a simultaneous approximation of both pressure head and velocity and can handle general irregular grids with highly heterogeneous permeability. However, for many problems dealing with unsaturated water flow, the MHFE solutions exhibit significant unphysical oscillations. To avoid this phenomenon, we develop an efficient mass-lumping scheme with the MHFE method for solving the mixed form of the Richards equation.

In this work, the standard and the lumped MHFE formulations are detailed and the ability of the lumped formulation to reduce unphysical oscillations is demonstrated for one and two dimensional infiltration problems. Theoretical analysis based on the *M*-matrix property, which guarantees the discrete maximum principle, and practical test cases carried out in this study, underline the interest of using an acute triangulation to completely remove the unphysical oscillations. Indeed, contrary to the standard approach, the lumped formulation satisfies the *M*-matrix property without any constraint on the time step size to be used.

Key words: Mixed finite element, unsaturated flow, the Richards equation, oscillations, mass-lumping.

Prediction of accurate fluid movement in porous media is an important issue for scientists and engineers who are interested in the management of water resources. Computational simulations have received much attention to achieve this predictive role. Even if its validity is still discussed the Richards equation (RE) is a valuable model to predict water movement and solute transport in variably saturated media (Simunek and Bradford, 2008).

From a mathematical point of view, the RE can be a highly nonlinear parabolic equation under unsaturated conditions, or a partial differential equation (PDE) of elliptic type for a fluid-saturated incompressible porous media. Among the various numerical schemes that can be used to solve the RE, the Mixed Finite Element (MFE) method is well suited for the discretization of elliptic and parabolic PDEs on heterogeneous domains. Moreover, it is locally conservative, can handle general irregular grids and allows a simultaneous approximation of both pressure and velocity.

Consequently, this method has been extensively employed during the last few years (Mosé et al., 1994; Bergamaschi et al., 1998; Younes et al., 1999; Ackerer et al., 1999; Chavent et al., 2003; Younes et al., 2006 among others). For practical applications, the lowest order mixed method of Raviart-Thomas (RT0) is frequently applied and is considered in this paper. RT0 uses a piecewise constant approximation for the pressure (Brezzi and Fortin, 1991). The velocity space has three degrees of freedom for triangular elements and four for quadrangular elements. In their original form, the mixed methods require the resolution of algebraic equations that typically lead to indefinite systems (Chavent and Jaffré, 1986; Brezzi and Fortin, 1991).

The most widely used approach to circumvent this mathematical difficulty is the hybridization technique (Roberts and Thomas, 1989). It consists in introducing pressure Lagrange multipliers at element edges. The Mixed Hybrid Finite Element (MHFE) method leads to a symmetric and positive definite matrix which generally does not satisfy the *M*-

matrix property (Raviart and Thomas, 1977; Thomas, 1977; Wheeler and Peszynska, 2002). This property (which requires a non singular matrix with $m_{ii} > 0$ and $m_{ij} \leq 0$) has nonetheless a nice physical impact, as the scheme in this case satisfies the discrete maximum principle, *i.e.* local maxima or minima will not appear in the numerical solution for a domain without local sources or sinks. Therefore, the resulting numerical state variable and its related fluxes are consistent with the physics.

For elliptic problems, the matrix obtained with MHFE is an *M*-matrix in the case of a weakly acute triangulation (all angles are less than $\pi/2$) (Brezzi and Fortin, 1991). This condition on angles is no more sufficient for parabolic problems. A first approach to preserve the *M*-matrix property is to change the RT finite element space for the flux variable (Marini and Pietra, 1990). Another way commonly used in finite element methods is mass-lumping (Segerlind, 1984). In the literature, a mass-lumping procedure is used with the MHFE method by using suitable quadrature formula in order to diagonalize the elemental matrix. This works nicely on rectangular meshes, where numerical quadrature makes the mixed approximation equivalent to finite differences (FD) (Weiser and Wheeler, 1988; Chavent and Roberts, 1991; Arbogast et al., 1998). An extension of this lumping procedure to triangular grids has been carried out in specific studies (Baranger et al., 1994; Sacco and Saleri, 1997; Micheletti and Sacco, 1999; Micheletti et al., 2001).

On the other hand, a new mass-lumping procedure, suitable for any shape of element, was developed in Younes et al. (2006) without any quadrature formulas. The basic idea of the method is (i) to calculate steady state fluxes using the standard MHFE method, and then (ii) to add the accumulation and sink/source terms directly on the edges where the MHFE method is seen as an edge/face centered finite volume method. This scheme was shown to be efficient to reduce unphysical oscillations for transient simulations of the saturated flow problem (Younes et al., 2006).

This article deals specifically with unsaturated flow and unphysical oscillations that can mainly appear ahead of sharp moisture fronts. Such numerical difficulties have been underlined for finite element (FE) (Milly, 1985; Celia et al., 1990; Pan et al., 1996; Ju et al., 1997; Karthikeyan et al., 2001) and MHFE (Farthing et al., 2003; Belfort and Lehmann, 2005) methods. Indeed, the nonlinear RE can be much more sensitive to unphysical oscillations and convergence problems may be encountered with the MHFE method.

The primary goal of this work is to describe how the mass-lumping formulation proposed in Younes et al. (2006) can be efficiently extended to the mixed form of the RE. Then, our objective is to show how the lumped formulation can improve the monotonicity and the efficiency of the MHFE method for unsaturated flow problems on general triangular and quadrangular meshes. Finally, numerical simulations are performed for 1D and 2D infiltration problems to show the benefit of the lumped MHFE formulation compared to the standard one.

VARIABLY SATURATED FLOW MODELING

Water flow in variably saturated porous media can be described by the Jacob – Richards equation which combines the mass conservation equation (1a) and the Darcy – Buckingham's law (1b) (Freeze, 1971; Narasimhan, 2004, 2006):

$$\begin{cases} (1a) \quad \dfrac{\partial \theta}{\partial t} + S_s S_w(\theta) \dfrac{\partial H}{\partial t} + \nabla . \vec{q} = f & in \quad \Omega \\ (1b) \quad \vec{q} = -K(h) . \nabla H & \\ H = H_e & on \quad \partial\Omega_D \\ -K(h) \dfrac{\partial H}{\partial \eta} = g & on \quad \partial\Omega_N \end{cases} \qquad [1]$$

where H and h are respectively the piezometric and pressure head such as $H = h + z$, z is the depth taken positive upward, S_s the specific storage coefficient, $S_w(=\theta/\theta_s)$ is the relative

saturation of the aqueous phase, θ the volumetric water content, θ_s the saturated water content, $\vec{q}$ the water velocity, f the source-sink term and K the hydraulic conductivity. Generally, on unsaturated conditions, the porous media and the fluid are assumed to be incompressible ($S_s = 0$). In this case, the Jacob-Richards equation reduces to the well known RE. In the rest of the paper, the equation [1] is referred to as RE.

The domain Ω is a bounded polygonal open set of $\mathbb{R}^2$, $\partial\Omega_D$ and $\partial\Omega_N$ are partitions of the boundary $\partial\Omega$ of Ω corresponding to Dirichlet and Neumann conditions, with either a fixed piezometric head H_e for Dirichlet boundaries or a fixed flux g for Neumann boundaries, and η the unit outward vector normal to the boundary $\partial\Omega$.

Equation (1a) can be written in several forms with either the water content and/or the pressure head as main unknowns. According to the chosen form, some care and specific adaptations have to be taken into account to conserve mass or to simulate variably saturated flow (Celia et al., 1990; Rathfelder and Abriola, 1994; Mansell et al., 2002).

The interdependencies of pressure head, hydraulic conductivity and water content are characterized using constitutive relations. According to recent studies (Vogel et al., 2001; Ippisch et al., 2006; Schaap and van Genuchten, 2006), the standard Mualem - van Genuchten model (Mualem, 1976; van Genuchten, 1980) has to be modified by adding an air entry value (h_e). The effective saturation is given by:

$$S_e = \begin{cases} = \dfrac{\theta - \theta_r}{\theta_s - \theta_r} = \dfrac{1}{S_E^*}\left[1 + \left(\alpha |h|\right)^n\right]^{-m}, & h < -h_e \\ 1, & h \geq -h_e \end{cases} \qquad [2]$$

where θ_s and θ_r are the saturated and residual volumetric water contents, respectively, α a parameter related to the mean pore size, n a parameter reflecting the uniformity of the pore-size distribution and $m = 1 - 1/n$.

The saturation at the cut-off point h_e is:

$$S_E^{\,*} = \left[1 + \left(\alpha h_e\right)^n\right]^{-m} \qquad [3]$$

The conductivity - saturation relationship becomes:

$$K\left(S_e\right) = \begin{cases} K_s S_e^{\,1/2}\left[\dfrac{1-\left(1-\left(S_E^{\,*} S_e\right)^{1/m}\right)^m}{1-\left(1-S_E^{\,*1/m}\right)^m}\right]^2, & S_e < S_E^{\,*} \\ K_s, & S_e \geq S_E^{\,*} \end{cases} \qquad [4]$$

where S_e is given by equation [2] and $n > 1$. K_s is the saturated conductivity (usually assumed as a scalar but could be a tensor for the general case).

Ippisch et al. (2006) show that the modified van Genuchten model is equivalent to the classical one for $n \gg 2$ and $\alpha h_e \ll 1$. Away from saturated conditions both models behave similarly.

NUMERICAL APPROACHES FOR SOLVING THE RICHARDS EQUATION

The standard MHFE method

In this work, the general mixed form of the RE is chosen because of many specificities to treat both water content and pressure head in the lumped MHFE formulation. Developments for the pressure head form of the RE can be easily deduced.

Discretization of the RE

The solution H of the system [1] is approximated over an element *E*, by the following quantities:

$H_E \in \mathbb{R}$: the mean value of H over the element E,

$TH_{E,i} \in \mathbb{R}$: the mean value of H over the edge E_i, [5]

$\overrightarrow{q_E} \in \overrightarrow{X_E}$: the approximation of $\vec{q} = -K(h)\nabla H$ over E.

where $\overrightarrow{X_E}$ is the lowest-order Raviart-Thomas space RT0 (Raviart and Thomas, 1977; Brezzi and Fortin, 1991; Chavent and Roberts, 1991) and $\overrightarrow{q_E}$ writes:

$$\overrightarrow{q_E} = \sum_{i=1}^{ne} Q_{E,i} \overrightarrow{\omega_{E,i}} \quad [6]$$

$Q_{E,i}$ denotes the flux leaving E through the i^{th} edge, taken positive outward and ne the number of edges of E ($ne = 3$ for a triangle and $ne = 4$ for a quadrangle).

The basis function $\overrightarrow{\omega_{E,i}}$ (see Fig. 1 in the case of a triangular element E) verifies (Brezzi and Fortin, 1991),

$$\int_{E_j} \overrightarrow{\omega_{E,i}} . \overrightarrow{\eta_{E_j}} = \delta_{ij} \quad [7]$$

$\overrightarrow{\eta_{E_j}}$ being the unit outward vector normal to the edge E_j of the element E.

The variational formulation of the flux law (1b) using [7] leads to:

$$\int_E K_E^{-1} \overrightarrow{q_E} \overrightarrow{\omega_{E,i}} = \sum_{j=1}^{ne} Q_{E,j} \int_E \overrightarrow{\omega_{E,i}} K_E^{-1} \overrightarrow{\omega_{E,j}} = -\int_E \nabla H \overrightarrow{\omega_{E,i}} = H_E - TH_{E,i} \quad [8]$$

where K_E is the value of the parameter K in the element E.

We introduce now local matrix notations on the element E:

$$M_{E,ij} = \int_E \overrightarrow{\omega_{E,i}} K_E^{-1} \overrightarrow{\omega_{E,j}} \quad [9]$$

The matrix M is symmetric and positive definite.

Equation [8] can be written as

$$Q_{E,i} = \sum_{j=1}^{ne} M_{E,ij}^{-1} \left(H_E - TH_{E,j} \right) = \alpha_{E,i} H_E - \sum_{j=1}^{ne} M_{E,ij}^{-1} TH_{E,j} \quad [10]$$

with $\alpha_{E,i} = \sum_{j=1}^{ne} M_{E,ij}^{-1}$.

Using a fully implicit time discretization and the property [7] of the RT0 basis functions, the mass balance equation (1a) takes the following discretized form:

$$|E|\left(\frac{\theta_E^{n+1} - \theta_E^n}{\Delta t^n} + S_s S_{w,E}^{n+1} \frac{H_E^{n+1} - H_E^n}{\Delta t^n} \right) + \sum_{i=1}^{ne} Q_{E,i}^{n+1} = |E| \, f_E^{n+1} \qquad [11]$$

where $|E|$ is the area of the element E, n the time level and Δt^n the time step size between the new and the old time levels $\left(\Delta t^n = t^{n+1} - t^n \right)$.

Due to the high non-linearities of the relationships between $h - \theta - K$, the water content is expanded using a first-order Taylor series with respect to the piezometric head (Celia et al., 1990):

$$\theta_E^{n+1,k+1} \simeq \theta_E^{n+1,k} + C_E^{n+1,k} \left(H_E^{n+1,k+1} - H_E^{n+1,k} \right) \qquad [12]$$

where C_E is the soil moisture capacity of the element E and k the iteration level.

Substituting equations [10] and [12] in equation [11] gives the mean piezometric head over the element *E*:

$$H_E^{n+1,k+1} = \frac{1}{\beta_E^{n+1,k}} \left[\sum_{i=1}^{ne} \left(\alpha_{E,i}^{n+1,k} T H_{E,i}^{n+1,k} \right) - \frac{|E|}{\Delta t^n} \left(\theta_E^{n+1,k} - C_E^{n+1,k} H_E^{n+1,k} - \theta_E^n - S_{S,E} S_{w,E}^{n+1,k} H_E^n \right) + |E| \, f_E^{n+1} \right] \qquad [13]$$

with

$$\begin{aligned} \beta_E^{n+1,k} &= \frac{|E|}{\Delta t^n} \left(C_E^{n+1,k} + S_{S,E} S_{w,E}^{n+1,k} \right) + \alpha_E^{n+1,k} \\ \alpha_E^{n+1,k} &= \sum_{i=1}^{ne} \alpha_{E,i}^{n+1,k} \end{aligned} \qquad [14]$$

According to this linearization strategy, equation [10] becomes:

$$Q_{E,i}^{n+1,k+1} = \sum_{j=1}^{ne} N_{E,ij}^{n+1,k} T H_{E,j}^{n+1,k+1} + F_{E,i}^{n+1,k} \qquad [15]$$

with

$$N_{E,ij}^{n+1,k} = \frac{\alpha_{E,i}^{n+1,k}\alpha_{E,j}^{n+1,k}}{\beta_E^{n+1,k}} - \left(M_{E,ij}^{n+1,k}\right)^{-1} \qquad [16]$$

and

$$F_{E,i}^{n+1,k} = \frac{\alpha_{E,i}^{n+1,k}}{\beta_E^{n+1,k}}\left(|E|\, f_E^{n+1} - \frac{|E|}{\Delta t^n}\left(\theta_E^{n+1,k} - C_E^{n+1,k}H_E^{n+1,k} - \theta_E^n - S_{S,E}S_{w,E}^{n+1,k}H_E^n\right)\right) \qquad [17]$$

Note that for general quadrangular elements, the local matrix $[N_E]$ cannot be evaluated easily and we resort to numerical integration. On the other hand, for triangular elements (see notations on Fig. 1), the matrix $[N_E]$ can be evaluated algebraically in the case of a scalar conductivity K_E (Younes et al., 2004),

$$\left[N_E^{n+1,k}\right] = -K_E^{n+1,k}\begin{bmatrix} \frac{r_{23}^{\,2}}{|E|} & -2\cot\left(\varphi_{E,12}\right) & -2\cot\left(\varphi_{E,13}\right) \\ -2\cot\left(\varphi_{E,12}\right) & \frac{r_{31}^{\,2}}{|E|} & -2\cot\left(\varphi_{E,23}\right) \\ -2\cot\left(\varphi_{E,13}\right) & -2\cot\left(\varphi_{E,23}\right) & \frac{r_{12}^{\,2}}{|E|} \end{bmatrix} - \frac{1}{3}\gamma_E^{n+1,k}\begin{bmatrix} 1 & 1 & 1 \\ 1 & 1 & 1 \\ 1 & 1 & 1 \end{bmatrix} \qquad [18]$$

in which r_{ij} is the edge vector from node i toward node j,

$$\gamma_E^{n+1,k} = \frac{K_E^{n+1,k}\left(\beta_E^{n+1,k} - \alpha_E^{n+1,k}\right)}{3K_E^{n+1,k} + \left(\beta_E^{n+1,k} - \alpha_E^{n+1,k}\right)\ell} \qquad [19]$$

and

$$\ell = \sum_{j=1}^{3} B_{ij} = \frac{\|r_{12}\|^2 + \|r_{23}\|^2 + \|r_{31}\|^2}{48|E|} \geq \frac{\sqrt{3}}{12}. \qquad [20]$$

The equation [15] is used to form the final system to solve. The scalar unknowns correspond to the mean piezometric head on the cell edges ($TH_{E,i=1,..,ne}$) and the final system of equations is obtained using continuity properties between adjacent elements:

- For all interior edges, the continuity of the normal component of the velocity and edge piezometric head between the two adjacent cells E and E' writes:

$$TH_{E,i} = TH_{E',j} \text{ and } Q_{E,i} + Q_{E',j} = 0, \quad [21]$$

- For a Dirichlet boundary edge E_i with a prescribed pressure TH_i^{bc}, we have:

$$TH_{E,i} = TH_i^{bc}, \quad [22]$$

- For a Neumann boundary edge with a given flux $Q_{N,i}$,

$$Q_{E,i} + Q_{N,i} = 0, \quad [23]$$

The resulting system matrix is symmetric and positive definite.

***M*-matrix condition for the standard MHFE formulation**

If a matrix is of type *M*, then it has a nonnegative inverse, i.e. all the elements of the inverse matrix are nonnegative. This implies the validity of the discrete maximum principle and thus monotonicity of the discretization. The *M*-matrix property requires a non singular matrix with positive diagonal entries and nonpositive off-diagonal entries.

In the case of the standard MHFE formulation, each line i of the global matrix represents the flux continuity between the two elements E and E' sharing the edge i, i.e. the sum of the two fluxes $Q_{E,i}$ and $Q_{E',j}$. Therefore, using [15], we can see that the global matrix is an *M*-matrix if both local matrices $\left[N_E\right]$ and $\left[N_{E'}\right]$ are of type *M*.

For one dimensional problems, it was shown in Belfort and Lehmann (2005) that $\left[N_E\right]$ is an *M*-matrix if the time size is larger than a critical value which depends mainly on soil moisture capacity and conductivity. For 2D rectangular meshes, the matrix $\left[N_E\right]$ can never be of type *M* (cf. Appendix). Finally, with triangular meshes, the matrix $\left[N_E\right]$ is an *M*-matrix if the triangulation is acute and if the time step is also great enough (cf. Appendix).

Note that criteria on the time step length may be difficult to respect in unsaturated conditions where conductivity, soil moisture capacity and saturation change at each iteration.

The Lumped MHFE method

Discretization of the RE

With the lumped formulation of the MHFE method, the stationary and the accumulation parts of the flux are distinguished (see Younes et al., 2006 for details) and it is written as:

$$Q_{E,i} = \overline{Q}_{E,i} + \frac{Q_{E,s}}{ne} - \frac{|E|}{ne}\left(\frac{\partial T\theta_{E,i}}{\partial t} + S_s S_w \frac{\partial TH_{E,i}}{\partial t} \right) \qquad [24]$$

where $Q_{E,s}$ is the sink/source term over the element E defined by $Q_{E,s} = \int_E f \, dE$ and $\overline{Q}_{E,i}$ is the flux corresponding to the stationary problem without sink/source terms. Notice that $\overline{Q}_{E,i}$ is given by equation [10]; but due to stationary conditions, the mean piezometric head H_E can be expressed only in terms of traces of piezometric heads $TH_{E,i=1,..,ne}$. The accumulation term of equation [24] is also expanded according to equation [12] with edge state variables.

Furthermore, using a fully implicit time discretization, we obtain (see Younes et al., 2006):

$$Q_{E,i}^{n+1,k+1} = \sum_{j=1}^{ne} N_{E,ij}^{n+1,k} TH_{E,j}^{n+1,k+1} + F_{E,i}^{n+1,k} \qquad [25]$$

where the local matrix $\left[N_E \right]$ obtained with the lumped formulation is given by,

$$N_{E,ij}^{n+1,k} = \frac{\alpha_{E,i}^{n+1,k} \alpha_{E,j}^{n+1,k}}{\alpha_E^{n+1,k}} - \left(M_{E,ij}^{n+1,k} \right)^{-1} - \lambda_{E,i}^{n+1,k} TH_{E,i}^{n+1,k+1} \delta_{ij} \qquad [26]$$

where

$$\alpha_E^{n+1,k} = \sum_{i=1}^{ne} \alpha_{E,i}^{n+1,k} \,, \qquad [27]$$

$$\lambda_{E,i}^{n+1,k} = \frac{|E|}{ne\Delta t^n}\left(TC_{E,i}^{n+1,k} + S_{S,E}S_{w,E,i}^{n+1,k}\right) \qquad [28]$$

and

$$F_{E,i}^{n+1,k} = \frac{|E|}{ne} f_E^{n+1} - \frac{|E|}{ne\Delta t^n}\left(T\theta_{E,i}^{n+1,k} - TC_{E,i}^{n+1,k}TH_{E,i}^{n+1,k} - T\theta_{E,i}^{n} - S_{S,E}S_{w,E,i}^{n+1,k}TH_{E,i}^{n}\right) \qquad [29]$$

The global lumped MHFE system matrix is also obtained using continuity of fluxes and traces of piezometric head between adjacent elements. The obtained matrix is also symmetric and positive definite.

M-matrix condition for the lumped MHFE formulation

As previously, the global *M*-matrix property is verified if the local matrix $\left[N_E\right]$ is of type *M*.

In the case for one-dimensional problems, the lumped formulation leads always to a local matrix of type *M* (Belfort and Lehmann, 2005). For 2D rectangular elements, as with the standard formulation, the *M*-matrix property can never be obtained (cf. Appendix).

Concerning triangular elements (see notations on Fig. 1), the local matrix [26] of the lumped formulation is given by:

$$\left[N_E^{n+1,k}\right] = -K_E^{n+1,k}\begin{bmatrix} \frac{r_{23}^{\,2}}{|E|} & -2\cot\left(\varphi_{E,12}\right) & -2\cot\left(\varphi_{E,13}\right) \\ -2\cot\left(\varphi_{E,12}\right) & \frac{r_{31}^{\,2}}{|E|} & -2\cot\left(\varphi_{E,23}\right) \\ -2\cot\left(\varphi_{E,13}\right) & -2\cot\left(\varphi_{E,23}\right) & \frac{r_{12}^{\,2}}{|E|} \end{bmatrix} - \begin{bmatrix} \lambda_{E,1}^{n+1,k} & 0 & 0 \\ 0 & \lambda_{E,2}^{n+1,k} & 0 \\ 0 & 0 & \lambda_{E,3}^{n+1,k} \end{bmatrix} \qquad [30]$$

Since $\lambda_{E,i}^{n+1,k}$ are all positive, the local matrix $\left[N_E\right]$ is always of type *M* for an acute triangulation. In this case and contrary to the standard MHFE scheme, the lumped formulation

allows to obtain a global *M*-matrix whatever the size of the time step (see Younes et al., 2006 and Appendix).

RESULTS AND DISCUSSION

Two numerical models based upon the standard and the lumped formulations of MHFE are developed for the resolution of the RE. Both use a linearization technique based upon the fixed point method (Picard Iteration) and an absolute convergence criterion function of the piezometric head variations. The codes can obviously be improved, for instance with a Newton Raphson linearization technique (Bergamaschi and Putti, 1999), with high order temporal approximations (Farthing et al., 2003), adaptive time stepping (Kavetski et al., 2001) or grid refinement (Mansell et al., 2002) techniques. However, these sophisticated strategies have not been investigated since we mainly focus in this work, on unphysical oscillation problems. Note that all theses techniques can easily be implemented with the lumped formulation of MHFE.

In the numerical codes, the hydraulic conductivity K_E of the element E is updated at each iteration using the arithmetic mean (Belfort and Lehmann, 2005):

$$K_E^{n+1,k} = \frac{1}{ne} \sum_{i}^{ne} K_E \left(Th_{E,i}^{n+1,k} \right) \qquad [31]$$

in which $Th_{E,i}^{n+1,k}$ is the mean pressure head over the edge E_i, given by

$$Th_{E,i}^{n+1,k} = TH_{E,i}^{n+1,k} - z_{E,i} \qquad [32]$$

Numerical experiments are performed with both codes to simulate infiltration of water in unsaturated porous medium (Celia et al., 1990). Parameters describing the soil are reported in Table 1. Since only unsaturated conditions are present in the domain, the air entry value and the storage coefficient have no significant effects and are fixed to zero. Furthermore, to

show the effect of the time step length on the unphysical oscillations, a fixed time strategy is adopted.

We simulate both 1D and 2D infiltration problems. Different spatial discretizations are studied in 2D (general quadrangular elements, general triangulation, Delaunay triangulation, acute triangulation). Parameters, initial and boundary conditions for both 1D and 2D problems are given in Table 1.

One-dimensional infiltration under a constant head boundary condition

The one dimensional infiltration problem is solved using a fixed time step of $\Delta t = 1\text{s}$ and different spatial discretizations (Δz varying from 1 cm to 6 cm).

A reference solution, which coincides with the quasi-analytical solution developed by Philip (1957), is evaluated numerically using small time step and nodal spacing (0.1s and 0.1 cm).

The wetting fronts after 6 hours of infiltration obtained with the standard and the lumped formulations are compared to the reference solution in Fig. 2. To obtain a good visual comparison of the MHFE schemes, results are given only for the upper 40 cm of the soil profile. Figure 2 shows clearly that the standard MHFE solution produces important unphysical oscillations. These undesired oscillations are eliminated with the lumped formulation of MHFE.

The computational efficiency of the proposed mass-lumping technique is verified by means of comparisons. Figure 3 represents the global error as a function of the global CPU time with mesh refinement (different Δz). The global error $GErr$ is defined by

$$GErr = \int_{z=0}^{z=L} \left| Th_{cal}(z) - Th_{ref}(z) \right| dz \Big/ \int_{z=0}^{z=L} \left| Th_{ref}(z) \right| dz \qquad [33]$$

where Th_{cal} is the edge value of pressure head (Eq. [32])calculated with a formulation of the MHFE method, and Th_{ref} is the reference pressure head obtained with a very fine grid system.

The results of Fig. 3 show that the lumped formulation is more efficient than the standard MHFE formulation. Indeed, in general, the lumped formulation requires 2.5 less CPU time than the standard one to achieve a fixed accuracy.

A 2D infiltration into initially dry soil

For this problem, we consider the infiltration of water into a $(50\,cm \times 100\,cm)$ rectangular domain. Boundary conditions are described in Table 1. All sides of the flow region were considered to be impervious, except for a strip of 20 cm length at the surface where ponded infiltration with 25 cm piezometric head was imposed. At the bottom, a prescribed piezometric head is fixed to a value of -1000 cm (see Fig. 4). The simulations are performed during one day. Four different spatial discretizations are used in this example: a general quadrangular mesh of 1250 cells (2575 edges), a general triangular mesh of 2500 cells (3825 edges), a Delaunay triangulation of 1716 cells (2632 edges) and an acute triangulation of 2048 cells (3136 edges). The general quadrangular mesh is depicted in Fig. 4. Simulations are carried out using either a small time step of 5s or a large time step of 200s and with both the standard and the lumped formulations of the MHFE method.

The expected numerical solution should be bounded. In this problem, the values of the piezometric head solution $TH_{E,i}$ at element edges should be between 25 cm (the upper Dirichlet boundary condition) and -1000 cm (the lower Dirichlet boundary condition). Because of the violation of the discrete maximum principle, the obtained numerical solution gives values less than -1000 cm. To quantify how badly the solution violates the maximum principle, we compute the minimal negative values of the solutions (H_{min}) as well as the relative sizes in % of the area where the maximum principle is violated,

$$\left(errg = \frac{\Omega\left(TH_E < -1000\,cm\right)}{\Omega} \right) \qquad [34]$$

Results of Table 2 show that strong unphysical oscillations appear with the standard MHFE method even with the large time steps $(\Delta t = 200s)$. Indeed the minimal values reach -1313.78 cm with quadrangles and about 12 % of the area can be concerned with unphysical oscillations. Similar unphysical results are obtained with the standard MHFE formulation for all kind of triangulations. If we reduce the time step size, the unphysical oscillations become more important and the nonlinear problem may not converge. Indeed, results with the standard formulation using a small time step of 5 s cannot be obtained since convergence problems are encountered with all meshes.

Results obtained with the lumped formulation are given in tables 3 and 4. Results with the large time step of 200 s show that the mass-lumping formulation allows a high reduction of the unphysical oscillations as compared to the standard approach. For the quadrangular mesh, the minimal value reaches -1022.90 cm and less than 3% of the area contain undesired oscillations. In the case of a general or a Delaunay triangulation less than 0.2% of the area is affected. The lumped formulation eliminates all unphysical oscillations when combined with an acute triangulation (Table 3).

Contrary to the standard formulation, the decrease of the time step size does not reduce the ability of the lumped formulation to solve the nonlinear problem. Results with the four discretizations are given in Table 4, when a small time step of 5 s is used. As with large time steps, the unphysical oscillations with the lumped formulation remain significant for quadrangles (minimal value -1028 cm). For triangular meshes, the unphysical oscillations are eliminated from the solution with the acute triangulation, but still exist for the general and Delanay triangulations (Table 4).

Recall that, Mazzia (2008) has recently shown that for the elliptic case with constant coefficients, the standard MHFE is monotonic for Delaunay-type meshes with the property that no circumcenters of boundary elements with Dirichlet conditions lie outside the domain.

Indeed, if we consider an interior edge i shared by two elements *E* and *F* (see Fig. 5), the Delaunay criterion can be written:

- for an interior edge i,

$$cot\,\varphi_{E,i} + cot\,\varphi_{F,i} > 0\,, \qquad [35]$$

- for a Dirichlet boundary edge j,

$$cot\,\varphi_{G,j} > 0\,, \qquad [36]$$

With the lumped formulation, the accumulation terms (terms with time derivative) are added only on the diagonal part. Therefore, the system matrix of the lumped formulation for the parabolic case should have the same behavior than the system matrix of the standard formulation for the elliptic case. The Delaunay criterion [35] - [36] is hence expected to be valid for transient simulations with the lumped MHFE formulation.

However, results of Tables 3 and 4 show that this criterion is not sufficient to avoid unphysical oscillations for the infiltration problem treated here. This occurs because the cotangent of the angles in the lumped formulation are always multiplied by conductivities (Eq. [30]). Therefore, the previous criteria are valid only in the homogeneous case. For heterogeneous porous media, [35] - [36] should be weighted by conductivities which lead to the following equations:

$$K_E\,cot\,\varphi_{E,i} + K_F\,cot\,\varphi_{F,i} > 0\,, \qquad [37]$$

$$K_E\,K_G\,cot\,\varphi_{G,j} > 0\,. \qquad [38]$$

In the case of unsaturated flow, K_E and K_F are nonlinear functions of the pressure head. According to the piezometric heads distribution and the flow process, the conductivity field can vary over several orders of magnitude. This situation is typically encountered for infiltration problems in dry soils. Therefore, even if [35] - [36] are verified, criteria [37] - [38] may not be fulfilled and the maximum principle is violated. On the other hand, for an acute

triangulation, [37] and [38] are always verified. In this case, the *M*-matrix property remains satisfied which guarantees the respect of the discrete maximum principle. This is shown numerically in Tables 3 and 4 where the results with the lumped MHFE formulation do not contain any unphysical oscillation.

For this 2D test case, the efficiency of the lumped formulation is demonstrated in Table 5 when simulations are achieved with a large time step of 200 s. The total computational time required can be compared for both methods. Results of this table show that the standard formulation requires between 15 % and 30 % more CPU time than the lumped one to perform the whole simulation. This increase in time is due to the increased effort required to iterate to reach a solution. Thus, because the monotonicity of the system is improved with the lumped formulation, the scheme is more efficient than the standard one.

A technique for improving the monotonicity with quadrangular elements

Results of Tables 3 and 4 show that in contrast to triangles, the unphysical oscillations with the lumped formulation remain significant with quadrangles (minimal value -1028 cm). Indeed it was shown in Younes et al. (2006) that the lumped formulation of MHFE can never give an *M*-Matrix even for an homogeneous problem with rectangular discretization.

To improve the monoticity of the lumped MHFE formulation for a general quadrangular mesh, we suggest in this part to change the local matrix of the quadrangles. The basic idea of this technique is to consider each quadrangular element *E* as an aggregation of two triangles *A* and *B* (Fig. 6).

Using equation [25] for each triangle, the fluxes $Q_{A,i}$ and $Q_{B,i}$ are only function of the edge piezometric heads $TH_{A,j}$ and $TH_{B,j}$. The continuity of the interior flux and the piezometric head between triangles *A* and *B* (see Fig. 6 for the notations and the numbering) is written:

$$Q_{A,3}^{n+1} + Q_{B,3}^{n+1} = \sum_{j=1}^{3} N_{A,3j}\, TH_{A,j}^{n+1} + F_{A,3}^{n+1} + \sum_{j=1}^{3} N_{B,3j}\, TH_{B,j}^{n+1} + F_{B,3}^{n+1} = 0$$
$$TH_{int}^{n+1} = TH_{A,3}^{n+1} = TH_{B,3}^{n+1} \qquad [39]$$

Since this interior piezometric head does not appear in our initial quadrangular discretization, the basic idea consists in simplifying the system related to the local triangulation by keeping only the piezometric head at the exterior edges, i.e. those of the quadrangular element *E*. To this aim, Eq. [39] provides an expression of the interior piezometric head,

$$TH_{int}^{n+1} = \frac{-1}{N_{A,33} + N_{B,33}} \left(\sum_{j=1}^{2} N_{A,3j}\, TH_{A,j}^{n+1} + F_{A,3}^{n+1} + \sum_{j=1}^{2} N_{B,3j}\, TH_{B,j}^{n+1} + F_{B,3}^{n+1} \right) \qquad [40]$$

Fluxes at exterior edges of the triangles are simplified by inserting Eq. [40] in Eq. [25]. This approach gives the expression of the fluxes $Q_{E,i}$ across edges of a quadrangular element *E* with a modified matrix N_E and a modified vector F_E. For instance, the flux across the first edge of the element E becomes:

$$Q_{E,1}^{n+1} = \left[N_{B,11} - \frac{N_{B,13} N_{B,31}}{N_{A,33} + N_{B,33}} \right] TH_{E,1}^{n+1} + \left[\frac{-N_{A,31} N_{B,13}}{N_{A,33} + N_{B,33}} \right] TH_{E,2}^{n+1} + \left[N_{B,12} - \frac{N_{B,13} N_{B,32}}{N_{A,33} + N_{B,33}} \right] TH_{E,3}^{n+1}$$
$$+ \left[\frac{-N_{A,32} N_{B,13}}{N_{A,33} + N_{B,33}} \right] TH_{E,4}^{n+1} - \frac{N_{B,13}}{N_{A,33} + N_{B,33}} \left(F_{A,3}^{n+1} + F_{B,3}^{n+1} \right) + F_{B,1}^{n+1} \qquad [41]$$

Using this formulation, it can be shown that the final system corresponds to an *M*-matrix if the fictitious triangulation is acute (angles of the triangles A and B are less than $\pi/2$).

This sub-discretization has the following advantages:

- The procedure can be applied only for some elements and not necessarily for the whole mesh. This is interesting for non-convex meshes which cannot be handled by the standard MHFE method. For example, the non-convex quadrangular element can be divided in two interior triangles (*A*, *B*) by dividing the greatest angle by 2.

- The parameters can change inside each quadrangle, which allows a better description of the spatial variability of the parameters without increasing the CPU time.
- The elemental matrix can be evaluated analytically without any quadrature formula even for distorted quadrangles.

- The developed approach has the same cost than the standard approach. In both formulations, the final system is solved for Lagrange multipliers at quadrangular edges.
- The monotonicity of the discretization is improved in order to avoid unphysical oscillations.
- The developed procedure is simple to implement (only the local matrix is changed).

Table 6 illustrates how the modified local matrix can improve the solutions of the lumped MHFE method for quadrangular meshes. Results demonstrate that the nonphysical oscillations are strongly reduced with the proposed technique since the minimal value decreases from -1028.01 cm to -1003.28 cm. The area affected by oscillations decreases also from 2.86% to 0.24%.

In this example, the unphysical oscillations are strongly reduced but not completely removed because the fictitious triangulation is not acute. In the case where the fictitious triangulation is acute, the maximum principle should be verified and oscillations can be completely removed with the proposed technique.

SUMMARY AND CONCLUSIONS

A lumped formulation of the MHFE method was developed for the resolution of the RE. Both standard and lumped formulations of MHFE were used to simulate infiltration problems in 1D and 2D with different time step sizes and different spatial discretizations.

The results of the infiltration problems may exhibit strong unphysical oscillations ahead of sharp moisture fronts. These oscillations are due to the violation of the maximum principle.

The numerical simulations show that:

1. For 1D infiltration problem, the lumped formulation allows to completely eliminate the unphysical oscillations that can appear with the standard approach;
2. For a general quadrangular mesh as well as for all kind of triangulations, strong unphysical oscillations appear in the solution obtained with the standard MHFE formulation. These oscillations increase with small time steps. In this case, convergence problems are encountered and the solution cannot be obtained;
3. The lumped formulation allows to strongly reduce these unphysical oscillations and results can be obtained even with small time steps. Contrarily to the standard formulation, in the case of acute triangulation, the lumped formulation gives an *M*-matrix which guarantees the maximum principle. Therefore, the unphysical oscillations are completely removed in this case;
4. The lumped formulation reduces the CPU time from 10 % to 22 % as compared to the standard formulation;
5. A sub-discretization technique has been proposed to improve the monotonicity of the solution for quadrangular meshes. Each quadrangle is considered as an aggregation of two triangles and a new local matrix for the quadrangle, based on

the local matrices of the triangles, is defined. This technique reduces the oscillation without decreasing the computational efficiency of the scheme.

Finally, we would like to underline that the improvements in the MHFE scheme through the mass-lumping technique depicted in this paper can be incorporated easily in multidimensional codes dealing with variably saturated flow.

ACKNOWLEDGMENTS

This work was partly supported by the GdR MoMas CNRS-2439 sponsored by ANDRA, BRGM, CEA and EDF whose support is gratefully acknowledged. The authors are also grateful to J. Nieber for several comments on this work and to the anonymous referees for their constructive remarks.

REFERENCES

Ackerer, Ph., A. Younes, and R. Mosé. 1999. Modeling variable density flow and solute transport in porous medium: 1. Numerical model and verification. Transp. Porous Media 35(3):345-373.

Arbogast, T., C. N. Dawson, P. T. Keenan, M. F. Wheeler, and I. Yotov. 1998. Enhanced cell-centered finite differences for elliptic equations on general geometry. SIAM J. Sci. Comput. 19(2):404-425.

Baranger, J., J.F. Maitre, and F. Oudin. 1994. Application de la théorie des éléments finis mixtes à l'étude d'une classe de schémas aux volumes-différences finis pour les problèmes elliptiques. C. R. Acad. Sci. Paris Sér. I Math. 401-404.

Belfort, B., and F. Lehmann. 2005. Comparison of equivalent conductivities for numerical simulation of one-dimensional unsaturated flow. Available at www.vadosezonejournal.org. Vadose Zone J. 4:1191-1200.

Bergamaschi, L., S. Mantica, and F. Saleri. 1998. A Mixed Finite Element - Finite Volume formulation of the black-oil model. SIAM J. Sci. Comput. 20 (3):970-997.

Bergamaschi, L. and M. Putti. 1999. Mixed finite elements and Newton-type linearizations for the solution of Richards' equation. Int. J. Numer. Methods Eng. 45:1025-1046.

Brezzi, F., and M. Fortin. 1991. Mixed and hybrid finite element methods. Springer-Verlag, Berlin.

Celia, M. A., E. T. Bouloutras, and R. L. Zarba. 1990. A general mass-conservative numerical solution for the unsaturated flow equation. Water Resour. Res. 26(7):1483-1496.

Chavent, G., and J. E. Roberts. 1991. A unified physical presentation of mixed, mixed hybrid finite elements and standard finite difference approximations for the determination of velocities in waterflow problems. Adv. Water Resour. 14:329-348.

Chavent, G., and J. Jaffré. 1986. Mathematical models and finite elements for reservoir simulation. North-Holland. Amsterdam.

Chavent, G., A. Younes, and Ph. Ackerer. 2003. On the Finite Volume Reformulation of the Mixed Finite Element Method for Elliptic and Parabolic PDE on triangles. Comput. Meth. Appl. Mech. Engrg. 192:655-682.

Farthing, M. W., C. E.Kees, and C. T. Miller. 2003. Mixed finite element methods and higher order temporal approximations for variably saturated groundwater flow. Adv. Water Resour. 26:373-394.

Freeze, R. A. 1971. Three-Dimensional, Transient, Saturated-Unsaturated Flow in a Groundwater Basin. Water Resour. Res. 7(2):347-366.

Ippisch, O., H.-J. Vogel, and P. Bastian. 2006. Validity limits for the van Genuchten-Mualem model and implications for parameter estimation and numerical simulation. Adv. Water Resour. 29:780-1789.

Ju, S. H., and K. J. S. Kung. 1997. Mass types, element orders and solution schemes for the Richards equation. Comput. Geosci. 23(2):175–87.

Karthikeyan, M., T.-S. Tan, and K. K. Phoon. 2001. Numerical oscillation in seepage analysis of unsaturated soils. Can. Geotech. J. 38:639–651.

Kavetsky, D., P. Binning, and S. W. Sloan. 2001. Adaptive time stepping and error control in a mass conservative numerical solution of the mixed form of Richards equation. Adv. Water Resour. 24(6):595-605.

Mansell, R. S., Ma. Liwang, L. R. Ahuja, and S. A. Bloom. 2002. Adaptive Grid Refinement in Numerical Models for Water Flow and Chemical Transport in Soil: A Review. Available at www.vadosezonejournal.org. Vadose Zone J. 1:222–238.

Marini, L. D., and P. Pietra. 1990. New mixed finite element schemes for current continuity equations. COMPEL 9(4):257-268.

Mazzia A. in press. An analysis of monotonicity conditions in the mixed hybrid finite element method on unstructured triangulations. Int. J. Numer. Methods Eng. DOI: 10.1002/nme.2330.

Micheletti, S., and R. Sacco. 1999. Stabilized mixed finite elements for fluid models in semiconductors. Comput. Visual. Sci. 2:139-147.

Micheletti, S., R. Sacco, and F. Saleri. 2001. On some mixed finite element methods with numerical integration. SIAM J. Sci. Comput. 23(1):245-270.

Milly, P. C. D. 1985. A mass-conservative procedure for time-stepping in models of unsaturated flow. Adv. Water Resour. 8:32-36.

Mosé, R., P. Siegel, P. Ackerer, and G. Chavent. 1994. Application of the mixed hybrid finite element approximation in a groundwater flow model: luxury or necessity?. Water Resour. Res. 30(11):3001-3012.

Mualem, Y. 1976. A new model for predicting the hydraulic conductivity of unsaturated porous media. Water Resour. Res. 12(3):513-522.

Narasimhan, T.N. 2004. Darcy's law and unsaturated flow. Available at www.vadosezonejournal.org. Vadose Zone J. 3:1059.

Narasimhan, T.N. 2006. On storage coefficient and vertical strain. Ground Water. 44(3):488-491.

Pan, L., A. W. Warrick, and P. J. Wierenga. 1996. Finite element methods for modelling water flow in variably saturated porous media: numerical oscillation and mass-distributed schemes. Water Resour. Res. 32(6):1883-1889.

Philip, J. R. 1957. Theory of infiltration: 1. The infiltration equation and its solution. *Soil Science* 83:435-448.

Rathfelder, K., and L. M. Abriola. 1994. Mass conservative numerical solutions of the headbased Richards equation. Water Resour. Res. 30(9):2579-2586.

Raviart, P. A. and Thomas, J. M., 1977. A mixed finite element method for second order elliptic problems. *In Mathematical Aspects of the finite elements method*, Vol.606, Magenes E, Springer, New York.

Roberts, J. E., and J. M. Thomas. 1989. Mixed and Hybrid methods, vol. II, Finite Elements Methods (part1), Ciarlet PG and Lions JL. North Holland. Amsterdam.

Sacco, R., and F. Saleri. 1997. Stabilized mixed finite volume methods for convection-diffusion problems. East West J. Numer. Math. 5(4):291-311.

Schaap M. G. and M. Th. van Genuchten. 2006. A Modified Mualem–van Genuchten Formulation for Improved Description of the Hydraulic Conductivity Near Saturation. Available at www.vadosezonejournal.org. Vadose Zone J. 5:27–34.

Segerlind, L. J. 1984. Applied Finite Element Analysis. 2nd ed. John Wiley & Sons.

Simunek, J. and S. A. Bradford. 2008. Vadose Zone Modeling: Introduction and importance. Available at www.vadosezonejournal.org. Vadose Zone J. 7:581–586.

Thomas, J. M. 1977. Sur l'Analyse Numérique des Méthodes d'Eléments Finis Hybrides et Mixtes. Ph.D. thesis Université Pierre et Marie Curie, France.

van Genuchten, M. Th. 1980. A closed-form equation for predicting the hydraulic conductivity of unsaturated soils. Soil Sci. Soc. Am. J. 44:892-898.

Vogel, T., M. Th. van Genuchten, and M. Cislerova. 2001. Effect of the shape of the soil hydraulic functions near saturation on variably-saturated flow predictions. Adv. Water Resour. 24(2):133-144.

Weiser, A., and M. F. Wheeler. 1988. On convergence of block-centered finite differences for elliptic problems. SIAM J. Numer. Anal. 25(2):351-375.

Wheeler, M. F., and M. Peszynska. 2002. Computational engineering and science methodologies for modeling and simulation of subsurface applications. Adv. Water Resour. 25:1147 – 1173.

Younes, A., P. Ackerer, and F. Lehmann. 2006. A new mass lumping scheme for the mixed hybrid finite element method. Int. J. Numer. Methods Eng. 67(1):89-107.

Younes, A., P. Ackerer, and G. Chavent. 2004. From mixed finite elements to finite volumes for elliptic PDEs in two and three dimensions. Int. J. Numer. Methods Eng. 59:365-388.

Younes, A., Ph. Ackerer, R. Mosé, and G. Chavent. 1999. A new formulation of the mixed finite element method for solving elliptic and parabolic PDE with triangular elements. J. Comput. Phys. 149:148-167.

APPENDIX

Local matrix $[N_E]$ for 2D rectangular element E :

MHFE (cf. Equation [16])	$\frac{3K_E^{\,2}}{K_E\left(\chi+\frac{1}{\chi}\right)+\frac{\gamma_E}{12}}\begin{bmatrix}\chi^2 & \chi^2 & 1 & 1\\ \chi^2 & \chi^2 & 1 & 1\\ 1 & 1 & 1/\chi^2 & 1/\chi^2\\ 1 & 1 & 1/\chi^2 & 1/\chi^2\end{bmatrix}-2K_E\begin{bmatrix}2\chi & \chi & 0 & 0\\ \chi & 2\chi & 0 & 0\\ 0 & 0 & 2/\chi & 1/\chi\\ 0 & 0 & 1/\chi & 2/\chi\end{bmatrix}$
LMHFE (cf. Equation [26])	$\frac{3K_E}{\left(\chi+\frac{1}{\chi}\right)}\begin{bmatrix}\chi^2 & \chi^2 & 1 & 1\\ \chi^2 & \chi^2 & 1 & 1\\ 1 & 1 & 1/\chi^2 & 1/\chi^2\\ 1 & 1 & 1/\chi^2 & 1/\chi^2\end{bmatrix}-2K_E\begin{bmatrix}2\chi & \chi & 0 & 0\\ \chi & 2\chi & 0 & 0\\ 0 & 0 & 2/\chi & 1/\chi\\ 0 & 0 & 1/\chi & 2/\chi\end{bmatrix}-\begin{bmatrix}\lambda_{E,1} & 0 & 0 & 0\\ 0 & \lambda_{E,2} & 0 & 0\\ 0 & 0 & \lambda_{E,3} & 0\\ 0 & 0 & 0 & \lambda_{E,4}\end{bmatrix}$
Notations	$\chi_E=\chi=\Delta z/\Delta x$ and $\gamma_E=\frac{\left(C_E+S_{s,E}S_{w,E}\right)\lvert E\rvert}{\Delta t}$

Conditions to satisfy M-matrix criterion for triangular elements:

Formulations	Conditions on angles	Condition on time step size
MHFE	$0\le\varphi_k\le 40.89°$	$tan\left(\varphi_k\right)-6\ell\le\frac{18K_E}{\gamma_E}$
LMHFE	$0\le\varphi_k\le 90°$	-
Notations	$\ell=\frac{\lVert r_{12}\rVert^2+\lVert r_{23}\rVert^2+\lVert r_{31}\rVert^2}{48\lvert E\rvert}$ (cf. Fig. 1) and $\gamma_E=\frac{\left(C_E+S_{s,E}S_{w,E}\right)\lvert E\rvert}{\Delta t}$	

List of Tables

Figure Captions

Table 1. Description of parameters and simulation conditions.

Variables		Values
Characteristics	θ_r (-)	0.102
	θ_s (-)	0.368
	α (cm^{-1})	0.033
	n (-)	2
	K_s ($cm.s^{-1}$)	9.22×10^{-3}
Dimensions	z (cm)	[0,100]
	x (cm)	[0,50]
Initial conditions		H (t = 0) = -1000 cm
Boundary conditions	upper	TH (z = 100, t) = 25 cm **(1D)**
		$TH(x, z = 100) = 25$ cm $\quad \forall x \in [0,20]$ $Q(x, z = 100) = 0$ $cm.s^{-1}$ $\quad \forall x \in]20,50]$ **(2D)**
	lower	TH (x, z = 0,t) = -1000 cm **(1D and 2D)**
	lateral **(2D)**	Q = 0 $cm.s^{-1}$

Table 2. Standard MHFE results with a large time step of 200 s.

	Quadrangles		General_triangles		Delaunay_triangles		Acute_triangles	
Time (s)	***err_g***	H_{min}	***err_g***	H_{min}	***err_g***	H_{min}	***err_g***	H_{min}
1600	9.34%	-1313.78	2.91%	-1171.42	2.96%	-1186.42	5.68%	-1273.77
7600	10.20%	-1246.62	3.72%	-1123.92	3.90%	-1100.46	8.69%	-1207.30
25000	11.90%	-1195.94	5.08%	-1116.42	4.75%	-1079.93	11.00%	-1168.23
36000	11.79%	-1151.03	4.79%	-1121.63	5.09%	-1000.11	11.00%	-1156.38
86400	10.82%	-1173.43	4.28%	-1114.14	5.06%	-1064.50	10.50%	-1110.57

Table 3. Lumped MHFE results with a large time step of 200 s.

	Quadrangles		General_triangles		Delaunay_triangles		Acute_triangles	
Time (s)	***err_g***	H_{min}	***err_g***	H_{min}	***err_g***	H_{min}	***err_g***	H_{min}
1600	1.34%	-1009.12	0.06%	-1000.039	0.02%	-1009.90	0.00%	-1000.00
7600	2.14%	-1007.58	0.04%	-1000.42	0.03%	-1000.02	0.00%	-1000.00
25000	2.83%	-1022.90	0.00%	-1000.00	0.09%	-1000.01	0.00%	-1000.00
36000	2.68%	-1022.35	0.10%	-1001.42	0.03%	-1000.11	0.00%	-1000.00
86400	1.98%	-1005.71	0.17%	-1003.08	0.00%	-1000.00	0.00%	-1000.00

Table 4. Lumped MHFE results with a small time step of 5 s.

	Quadrangles		General_triangles		Delaunay_triangles		Acute_triangles	
Time (s)	***err_g***	H_{min}	***err_g***	H_{min}	***err_g***	H_{min}	***err_g***	H_{min}
1600	1.11%	-1011.16	0.04%	-1000.032	1.49E-04	-1009.70	0.00%	-1000.00
7600	2.02%	-1007.02	0.04%	-1000.33	2.61E-04	-1000.01	0.00%	-1000.00
25000	2.86%	-1028.01	0.03%	-1000.02	9.06E-04	-1000.02	0.00%	-1000.00
36000	2.64%	-1024.43	0.10%	-1001.78	0.03%	-1000.11	0.00%	-1000.00
86400	1.90%	-1005.72	0.17%	-1003.28	0.00%	-1000.00	0.00%	-1000.00

Table 5. Total CPU time (s) with the standard and the lumped MHFE formulations.

	Quadrangles	General_triangles	Delaunay_triangles	Acute_triangles
MHFE	108.28	152	99.79	124.35
Lumped MHFE	89.33	131	79.43	96.25

Table 6. Results with the lumped MHFE and a small time step of 5 s.

	Quadrangles with Standard local matrix		Quadrangles with the modified local matrix	
Time (s)	***err_g***	H_{min}	***err_g***	H_{min}
1600	1.11%	-1011.16	0.07%	-1000.03
7600	2.02%	-1007.02	0.09%	-1000.33
25000	2.86%	-1028.01	0.03%	-1000.02
36000	2.64%	-1024.43	0.15%	-1001.78
86400	1.90%	-1005.72	0.24%	-1003.28

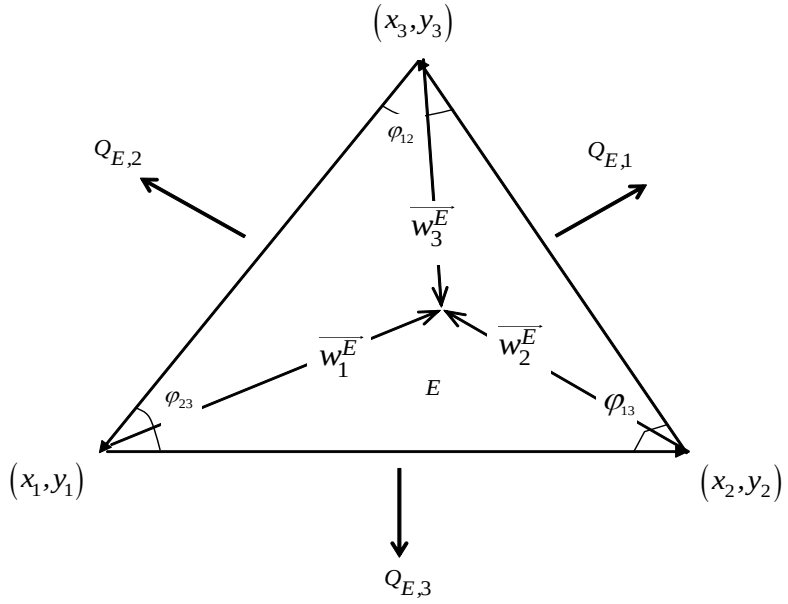

Fig. 1. Vectorial basis functions with RT0 on triangles.

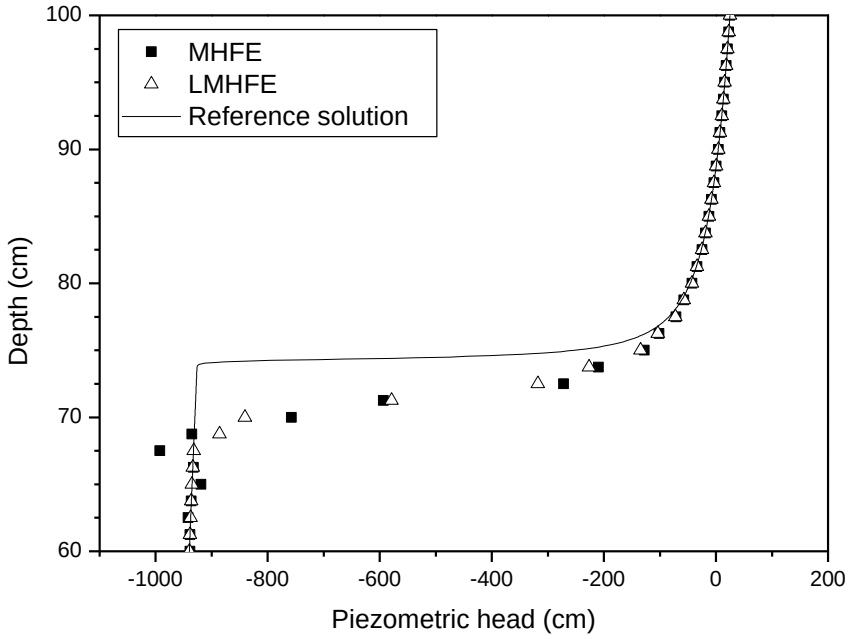

Fig. 2. Illustration of infiltration front for the upper 40 cm of the soil with $\Delta z = 2.5$ cm.

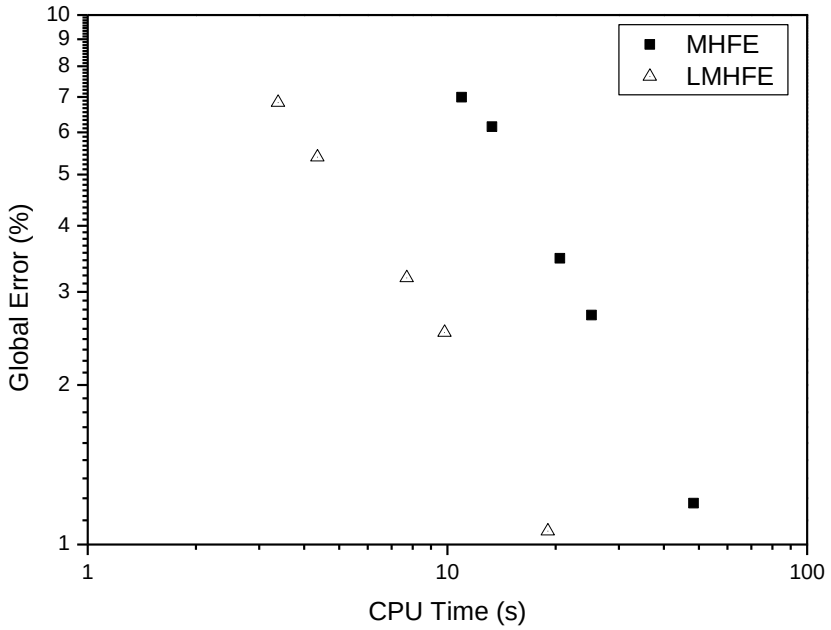

Fig. 3. Global error versus CPU time for various MHFE formulations and nodal spacing.

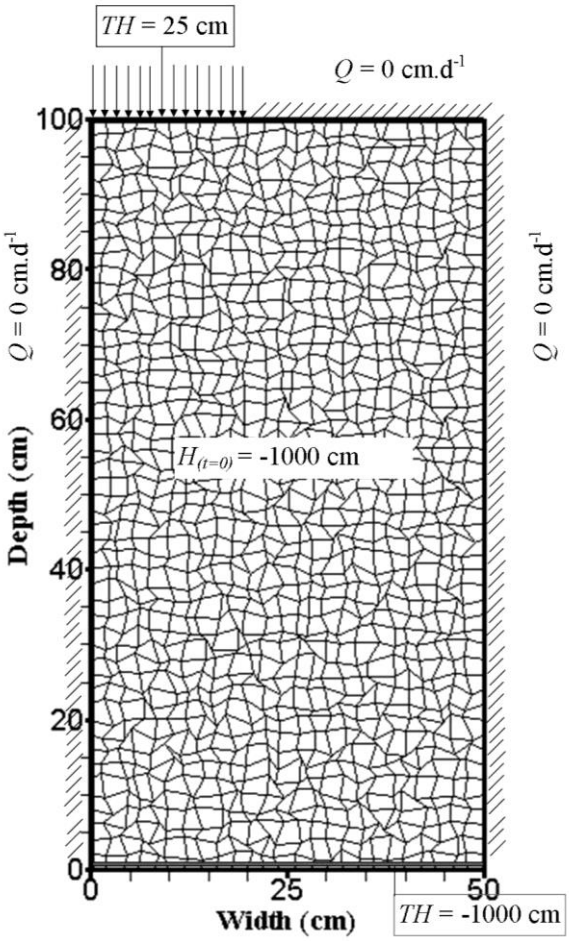

Fig. 4. Illustration of the 2D test case.

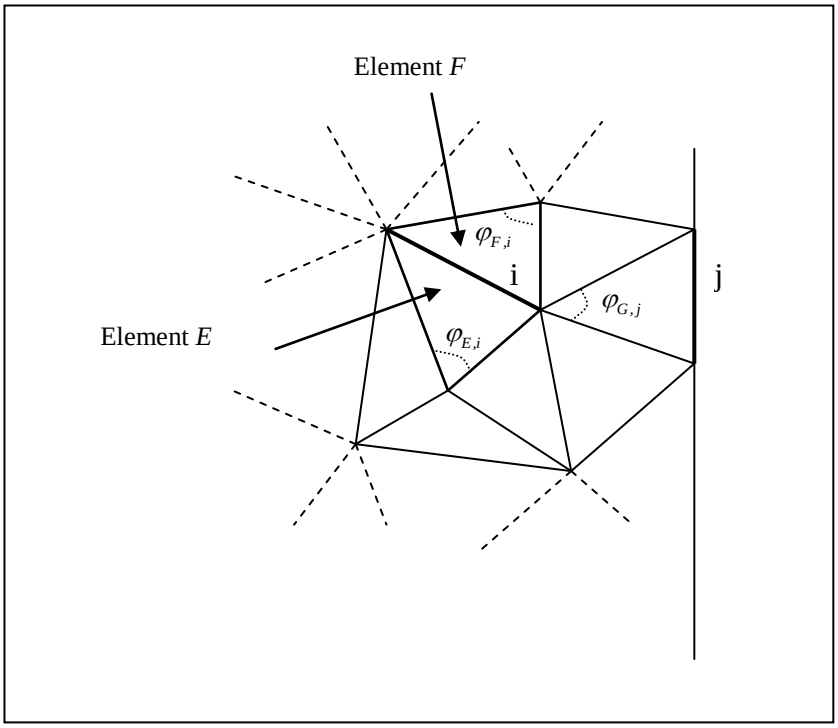

Fig. 5. Illustration of Delaunay criterion.

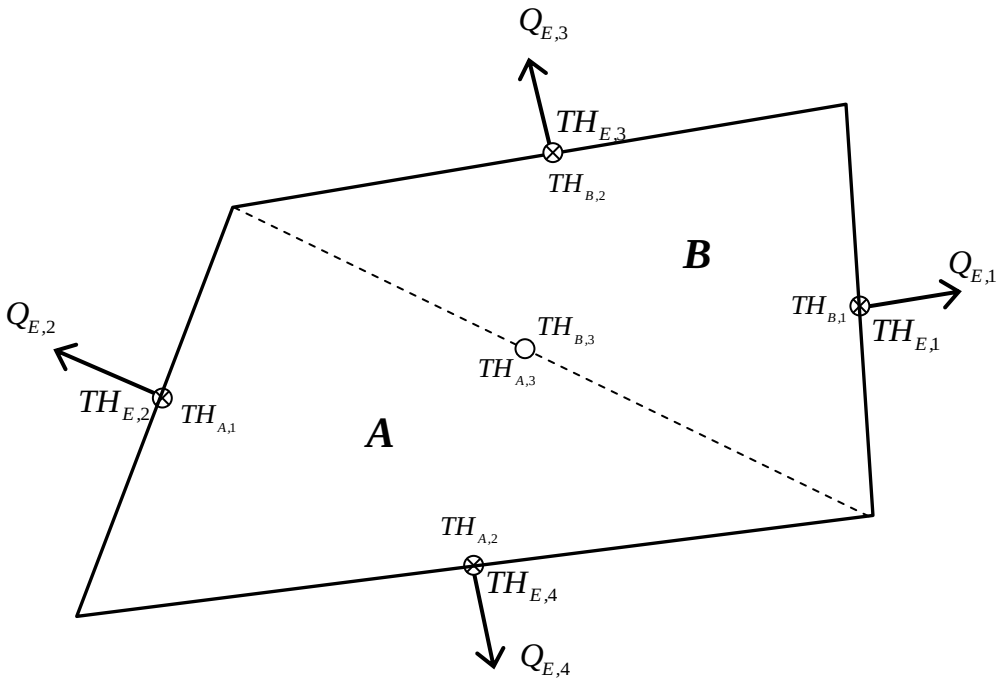

Fig. 6. Subdivision of a quadrangular cell E into 2 triangular elements A and B.